# BLADE PRESSURE LOADING AND TORQUE MEASUREMENT IN A TRANSONIC LINEAR CASCADE

**Jan Lepicovsky, David Šimurda, Jindřich Hála**
Institute of Thermomechanics, Czech Academy of Sciences, Dolejškova 5, Prague, Czech Republic

**Petr Šidlof, Martin Štěpán**
Technical University of Liberec,
Studentská 2, Liberec, Czech Republic

## ABSTRACT

Experimental results of a transonic compressor blade pressure loadings and blade shaft torque measurements are presented in this paper. Data were acquired for the cascade middle blade being set to a number of incidence angle offsets to simulate phases of a blade flutter oscillatory motion. This paper should be viewed as a progress report on the ongoing larger research effort on blade flutter in transonic flow regimes.

## NOMENCLATURE

| | | |
|---|---|---|
| $c$ | [m] | blade chord |
| $f_b$ | [Hz] | oscillation frequency |
| $Ma_1$ | [1] | inlet Mach number |
| $Ma_x$ | [1] | blade surface local Mach number |
| $p_{1t}$ | [kPa] | inlet flow total pressure |
| $p_W$ | [kPa] | cascade wall average pressure |
| $p_x$ | [kPa] | blade surface local pressure |
| $p_y$ | [kPa] | cascade wall local pressure |
| $p(t)$ | [kPa] | blade local unsteady pressure |
| $t$ | [ms] | time |
| $W$ | [m] | cascade width |
| $x$ | [m] | horizontal distance |
| $y$ | [m] | vertical distance |
| $\varepsilon$ | [deg] | incidence angle offset |
| $\mu$ | [Nm] | blade static torque |
| $\sigma$ | [kPa] | pressure standard deviation |

## INTRODUCTION

Striving for higher performance and enhanced machine operation flexibility of newly designed turbomachines will augment undesired flutter phenomena in stages with long slender blades. There is still no reliable methodology assuring that newly designed turbomachines will not experience blade flutter events while operated at off-design conditions. Experimentally determined unsteady blade loading functions are needed at the onset of a design cycle to shorten its length and improve its effectiveness. However, obtaining the needed blade loading functions on real turbomachines is extremely complicated and prohibitively expensive. Consequently, most of the experimental research is carried on using simplified dedicated test facilities, predominantly linear or arch segment blade cascades (Buffum and Fleeter, 1990; Vogt and Fransson, 2002; Fransson and Vogt, 2003). Although, such facilities are limited substitutions for "infinite" circular cascades of real turbomachines due to the linear cascade end effects, there are dynamic interaction effects between oscillating blades and transonic flow that can be reliably investigated in such facilities. The Institute of Thermomechanics of the Czech Academy of Sciences instigated an advanced research program on blade flutter research in order to enhance the understanding of blade flutter onset conditions for off-design operation regimes.

## BLADE FLUTTER MODULE

A new innovative test facility, Blade Flutter Module (BFM), for forced flutter research in transonic flow regimes was designed and built in the High-Speed Laboratory of the Institute of Thermomechanics (IT CAS). The BFM test section consists of five blades arranged in a linear cascade. The cascade flow channel height is 195 mm and its width is 160 mm. A layout of the blades in the test cascade is shown in Figure 1; the blade chord is 120 mm and the cascade blade pitch is 74.5 mm. The selected airfoil profile was developed for a research transonic compressor rotor by Schreiber and Starken (1984). The cascade stagger angle is 38.5 deg. The self-contained BFM module was installed in the IT CAS transonic suck-down wind tunnel (Lepicovsky et al., 2020). An overall view of the assembled test facility is in Figure 2.

The test module can be operated either in a static or a dynamic regime. No blade is oscillated for the static operation regime. Any of the blades can be manually set to a fixed incidence angle offset of up to +/-3 deg to simulate the maximum blade deflection during flutter oscillations. For the dynamic operation, any of the blades can be oscillated independently at frequencies of up to

400 Hz, with the maximum angular amplitude of 3 deg (Lepicovsky et al., 2022). Three of the five blades were densely instrumented with conventional static taps as well as with miniature pressure transducers. The instrumentation trenches on the airfoils were made on the blade passive side. Consequently, there are only 0.5 mm taps on the active side of the blade that do not disturb the flow in the boundary layer. It is quite a challenge to insert miniature pressure transducers in thin airfoils. The transducers were inserted with sensing diaphragms oriented in the plane perpendicular to the blade pitching axis to eliminate distortion of pressure signals by acceleration effects (Lepicovsky, 2005).

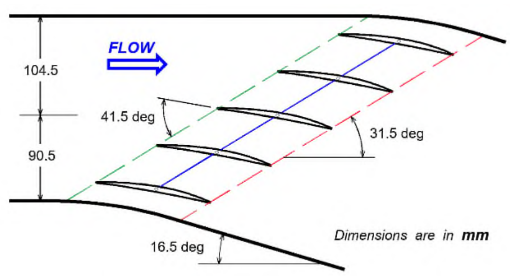


**Figure 1 Test cascade layout.**

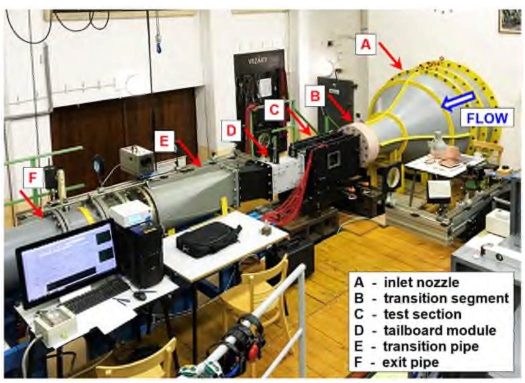


**Figure 2 View of test facility.**

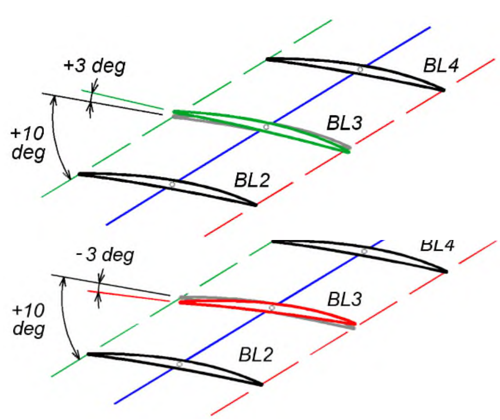


**Figure 3 Maximum positive and negative incidence angle offsets (BL3).**

## WORK OBJECTIVE AND PROGRESSION

A blade deflects periodically from a design incidence angle once the flutter oscillatory motion is set in force. Obviously, the oscillating blade alters the surrounded flowfield in the two following ways. First, it is a variation of the flow passage geometry due to the periodic changes of the blade incidence angle, and second, it is periodic fluid compression and expansion in the blade neighbourhood due to the blade piston-like motion. The primary objective of the current research effort is to explore contributions of the incidence offset effects to the resulting overall dynamic effects on the periodic loading of an oscillating blade. The experiments were carried out for a range of inlet Mach numbers from 0.70 up to 1.09. However, as the main focus is on transonic flow regimes, only data for the inlet Mach numbers of 0.90 and 1.09 are presented here. A character of the blade loading function is largely determined by the blade suction-side pressure distribution. Therefore, data presented in this paper are mostly for the airfoil suction side. The effects of static incidence offsets were determined by setting the middle blade to a range of incidence angles while the facility was operated with no oscillating blade. Then, the middle blade instrumented with miniature pressure transducers was oscillated up to 200 Hz for the dynamic regime data. Only the time-averaged values of measured unsteady pressure data and their comparison with the static data are presented in this paper. However, the local standard deviations of unsteady data along the blade suction surface are presented. An introductory phase of numerical modelling in 3D was also carried out (Hála et al., 2022). Finally, a measurement of the applied aerodynamic torque for various inlet flow conditions and incidence angle offsets was performed for the middle blade BL3.

## EFFECTS OF INCIDENCE ANGLE OFFSET

A blade periodic flutter motion can be stroboscopically fragmented into a series of positions for various incidence angle offsets to investigate the effects of flow-passage variation on blade loading. The incidence offset effects were investigated by setting the middle blade incidence angle to offsets of up to +/- 3 deg. The maximum blade incidence offsets are depicted in Figure 3. The effects of the blade BL3 incidence changes were detected in the static wall pressure distribution upstream of the cascade. However, as shown in Figures 4 and 5 only the flow region of blade BL4 was affected.

The results of blade pressure loadings for the inlet Mach number of 0.90 for the incidence angle offset range of +/- 3 deg are shown in Figure 6. The incidence effects are evident in the front half of the blade. Decreasing the blade incidence (negative incidence offset) slightly and smoothly

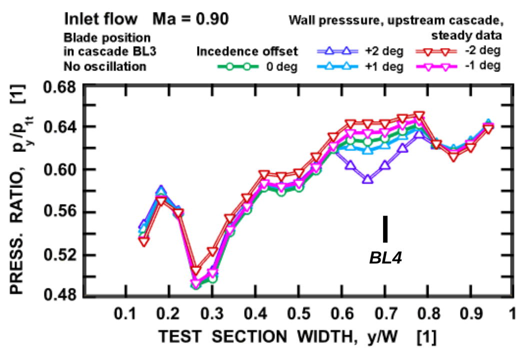


**Figure 4 Upstream cascade wall pressure distributions for subsonic inflow and changing incidence offsets.**

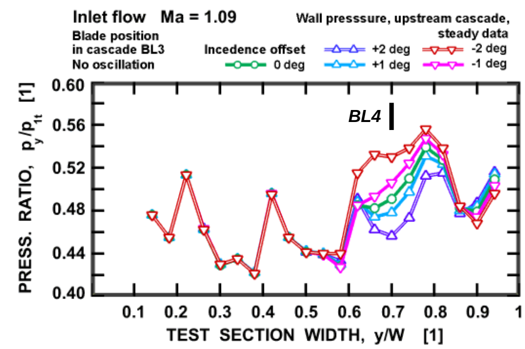


**Figure 5 Upstream cascade wall pressure distributions for supersonic inflow and changing incidence offsets.**

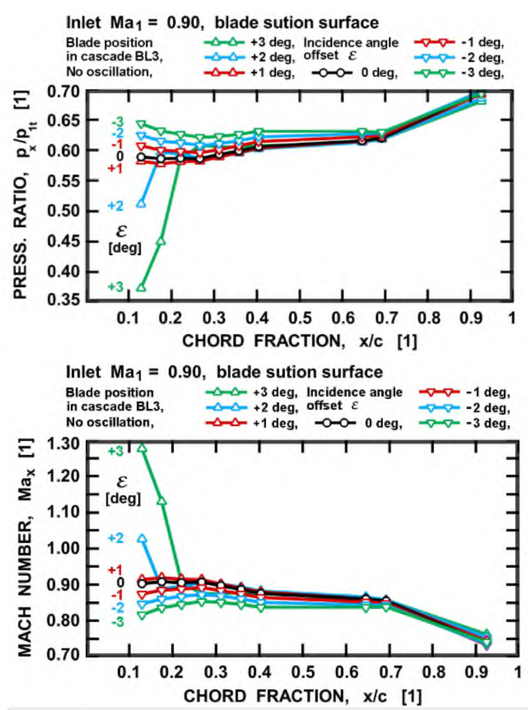


**Figure 6**
**Pressure distributions and Mach numbers on suction side of blade BL3 for subsonic inflow and changing incidence angle offsets.**

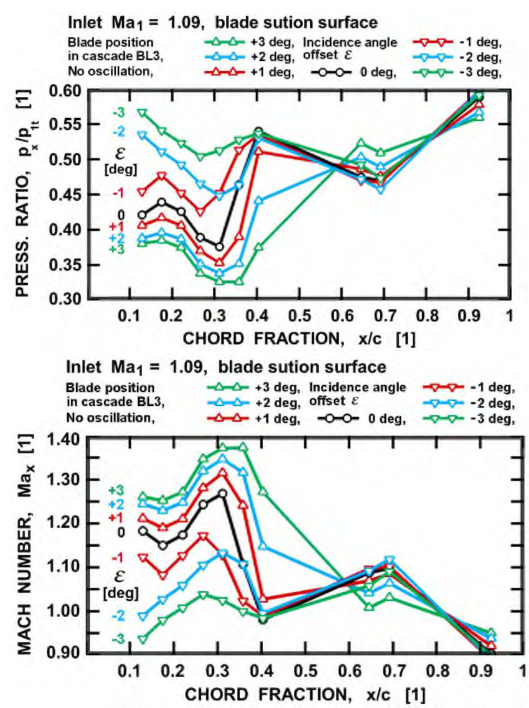


**Figure 7**
**Pressure distributions and Mach numbers on suction side of blade BL3 for supersonic inflow and changing incidence angle offsets.**

decreases the blade loading. However, for increasing the blade incidence, namely above 1 deg, the increase in the blade loading is hugely increased in the first 20 % of the blade chord. Obviously, the flow in that region is accelerated above the speed of sound and the region ends with a closing shock wave. Changes in the blade loading for the supersonic inlet Mach number of 1.09 are vividly different as shown in Figure 7. The flow stays supersonic over the 40 % of the blade chord except of the frontier values at the incidence offset of -3 deg. A strong shock wave closes the supersonic region. The shock wave intensity stays the same for the negative incidence offsets and then starts to decrease with an increasing positive incidence offset. The presented data document an enormous change in the blade loading while the cascade inlet flow passes through the transonic conditions. It should be stressed that the presented changes are due only to the changes in the flow passage geometry during the simulated motion period between the upper and lower blade oscillation dead centres.

The blade suction-side pressure loading was numerically modelled for both inlet Mach numbers for the blade set at the nominal incidence angle of 10 deg. The blade cascade was numerically modelled in 3D using the system of time-averaged Navier-Stokes equations for compressible flow complemented with the equation of state of an ideal gas. The Reynolds stress tensor and the turbulent thermal diffusivity were computed using the k-ω SST turbulence model. The inviscid fluxes were approximated using the Advection Upstream Splitting Method (AUSM) upwind scheme with linear reconstruction. The steady state solution was obtained using the density-based implicit solver in Ansys Fluent commercial code employing second order accuracy upwind schemes in space. The computational domain was symmetric in the span-wise direction; therefore, a symmetry boundary condition was used in the mid plane. At the outlet, the average static pressure was set to obtain desired inlet Mach number. The results are presented in Figures 8 and 9. There is a discrepancy between the computational predictions and the experimental results; nevertheless, the basic features of the CFD simulation and the experimental data are similar to a degree. It is particularly true for the supersonic inlet flow. The local shock indicated in the CFD data for the subsonic inlet Mach number is probably a consequence of an overestimated averaged inlet flow Mach number based on a nonuniform wall pressure distribution upstream of the cascade (see Figure 4).

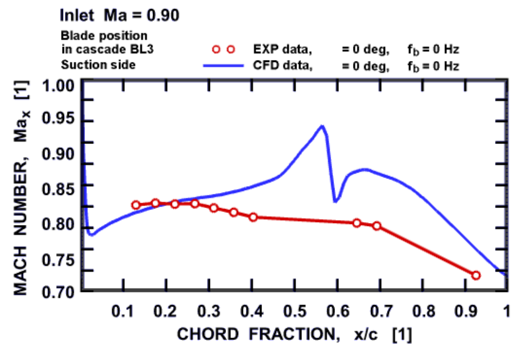


**Figure 8 CFD modelling and experimental data for subsonic inlet flow.**

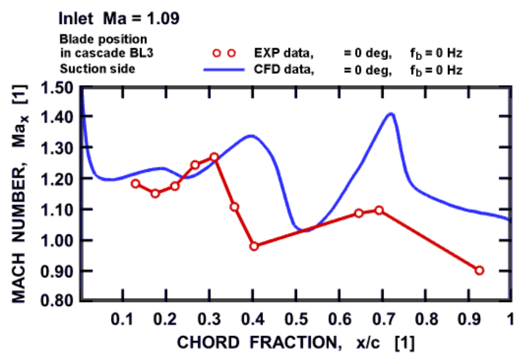


**Figure 9 CFD modelling and experimental data for supersonic inlet flow.**

## DYNAMIC LOADING EFFECTS

The overall dynamic effects on the periodic blade loading can be determined from unsteady pressure measurements along the suction surface on an oscillating blade. Examples of recorded unsteady pressure data are in Figures 10 and 11. Data in these figures are for the inlet Mach numbers of 0.90 and 1.09, and the oscillation frequency of 120 Hz. Segments of recorded unsteady pressures are for three stations along the blade chord, namely for x/c = 0.193, 0.348, and 0.883. For the subsonic inlet flow, the induced amplitude of pressure fluctuations at the blade front is 2.0 kPa (Figure 10a), slightly increases to 2.5 kPa further downstream (Figure 10b), and then drops to 1.0 kPa at the blade tail (Figure 10c). It appears that an additional lower frequency is induced at the blade rear section.

In short, the amplitude of the induced pressure fluctuations stays practically the same over the front half of the blade and then decays toward the end of the blade chord. However, for the supersonic inlet flow the situation is very different. Though the induced pressure amplitude is initially the same as for the subsonic case (Figure 11a), there are occasional instances of a strong shock wave passing upstream of the measurement station causing huge pressure spikes on the order of 10 kPa. Further downstream the shock wave intermittency locks into the oscillation frequency causing local pressure fluctuations of an amplitude of 6 kPa (Figure 11b). Occasionally, the shock does not cross the measurement station and in that case the induced pressure amplitude stays at the pre-shock level. Finally, towards the blade trailing edge the induced pressure fluctuations fade out (Figure 11c). This activity is best summarized in the distribution of pressure standard deviations along the blade chord shown in Figure 12. As seen here, the pressure standard deviation does not change along the blade suction side for the subsonic inlet flow. However, for the supersonic inlet flow there is a huge peak of the standard deviation at the 40 % of the blade chord length.

## BLADE TORQUE MEASUREMETS

A turbomachine blade in flutter is subjected to combined static and dynamic torque loadings. The static torque component is imposed by the surrounding flow on the blade that is not oscillating. The dynamic loading component is caused by an acceleration force on the oscillating blade in no flow environment. Measurement of blade static torque loading was carried out during the initial phase of this research project. Shafts of three middle blades were instrumented with strain gauges to detect torque moments being inserted on the blades. A view of the instrumented shafts is in Figure 13. Torque measurements were carried out for two inlet Mach numbers of 0.90 and 1.09. The middle blade (BL-3) was gradually set to incidence angle offsets

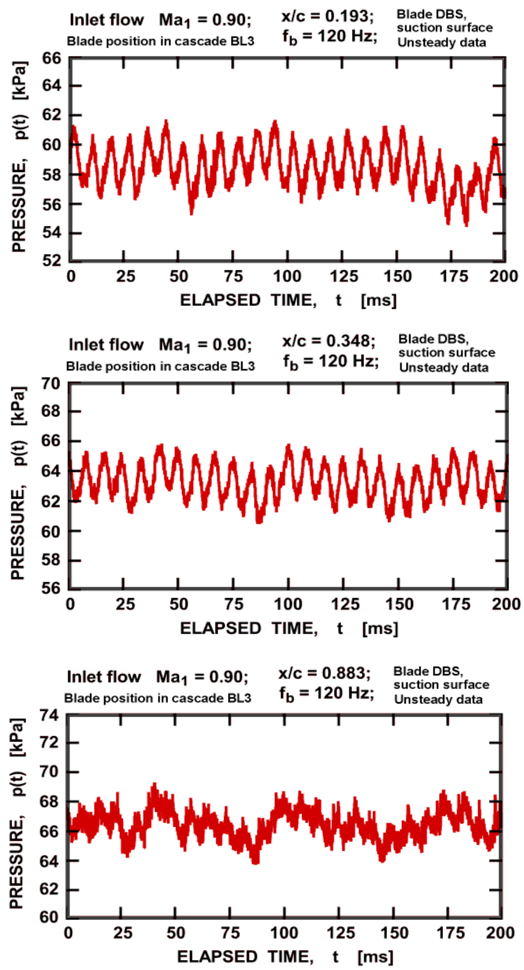


**Figure 10**
**Segments of recorded unsteady pressure on suction side of blade BL3 for forced blade oscillation at 120 Hz and subsonic inlet flow (A: x/c = 0.193; B: x/c = 0.348; C: x/c = 0.883)**

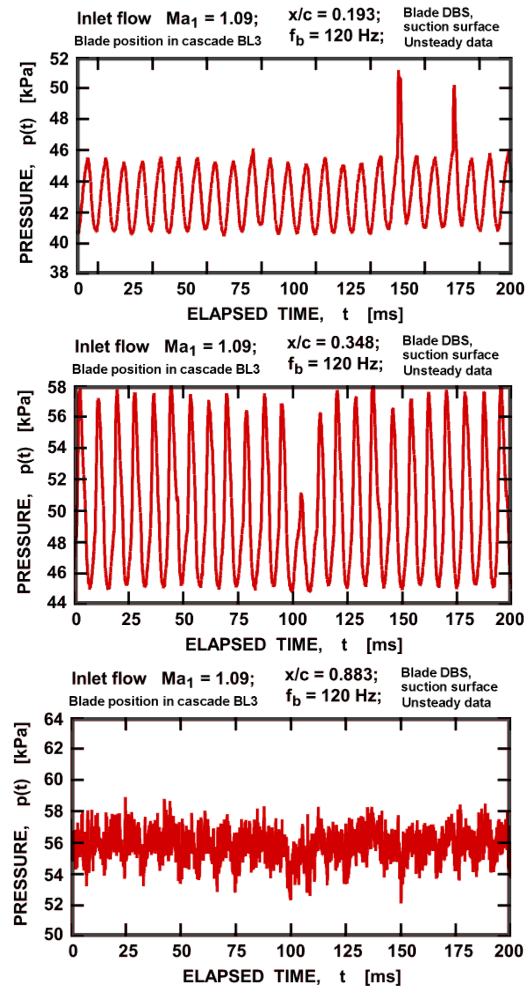


**Figure 11**
**Segments of recorded unsteady pressure on suction side of blade BL3 for forced blade oscillation at 120 Hz and supersonic inlet flow (A: x/c = 0.193; B: x/c = 0.348; C: x/c = 0.883)**

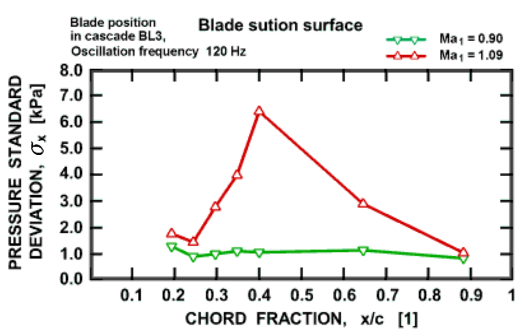


**Figure 12 Distributions of unsteady pressure standard deviations along the blade suction surface for subsonic and supersonic inlet flows.**

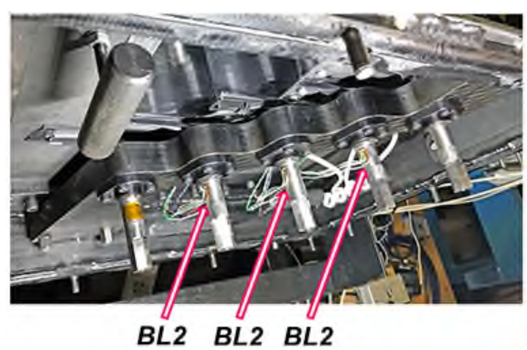


**Figure 13 View of blade shafts instrumented with strain-gauges for torque measurements.**

from -3 deg through +3 deg for repetitive torque data acquisitions. The results of static torque measurements on the middle blade BL3 are presented in Figure 14. As seen here, the static torque loading is a strong function of the blade incidence offset. It increases monotonically with an increasing incidence offset angle. It appears that there is no static torque loading difference between the subsonic and supersonic inlet flow regimes within a narrow incidence offset range of 1 deg around the design incidence angle.

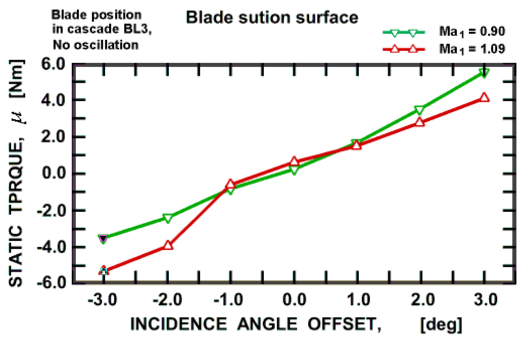


**Figure 14**
**Static torque loadings of cascade middle blade (BL3) as functions of blade incidence angle offsets for subsonic and supersonic inlet flows.**

## SUMMARY OF RESULTS

Several main results were accomplished during this phase of this research work. The newly built test facility for forced blade flutter research is fully operational and is available for future use. A series of test runs simulating blade flutter conditions were carried out for the range of inlet transonic Mach number in arrange between 0.90 and 1.09, and blade oscillation frequencies up to 200 Hz. Blade instrumentation with miniature pressure transducers prove to be reliable and free of the acceleration signal distortions. Blade static torque measurement was also successfully accomplished. Computational simulation of the blade loading will require a more detail modelling of the nonuniform cascade inlet flow conditions. The most significant achievement is the creation of an extensive base of experimental data for the transonic flow conditions available for general use.

## ACKNOWLEDGEMENTS

The project was supported by Ministry of Education, Youth and Sports of the Czech Republic under grant no. LTAUSA19036. Institutional support of the Institute of Thermomechanics of the Czech Academy of Sciences RVO:61388998 is also gratefully acknowledged.

## REFERENCES

Buffum, D.H. and Fleeter, S. (1990), “Aerodynamic of a Linear Oscillating Cascade”, NASA TM-103250.

Fransson, T.H. and Vogt, D.M. (2003), “A New Facility for Investigating Flutter in Axial Turbomachines”, Paper at the 8th National Turbine Engine High Cycle Fatigue Conference, Monterey, California, U.S.A.

Hála, J., Lepicovsky, J., Šidlof, P. and Šimurda, D. (2022), “CFD Investigation of the test facility for forced blade flutter research”, EPJ Web of Conferences 264,01017.

Lepicovsky, J., Šidlof, P., Šimurda, D., Štěpán, D. and Luxa M. (2020), “New Test Facility for Forced Blade Flutter Research”, XIX International Conference Power System Engineering, PSE 2020, p. 20, Pilsen.

Lepicovsky, J., Šimurda, D., Šidlof, P. and Luxa M. (2022), “Exploratory Experiments for Simple Approximation of Blade Flutter Aerodynamic Loading Function”, Paper GT2022-83351, Proceedings of ASME Turbo Expo 2022.

Schreiber, H.A. and Starken, H. (1984), “Experimental Cascade Analysis of a Transonic Compressor Rotor Blade Section”, J. of Eng. for Gas and Power, vol. 106, pp. 288-294.

Vogt, D.M. and Fransson, T.H. (2002), “A New Turbine Cascade for Aeromechanical Testing”, Paper at the 16th Symposium on Measuring Techniques in Transonic and Supersonic Flows in Cascades and Turbomachines, Cambridge, UK.